The Journal of Clinical Pharmacology 54(10) 1097–1107

DOI: 10.1002/jcph.304

Pharmacokinetics and Pharmacodynamics of *nab*-Paclitaxel in Patients With Solid Tumors: Disposition Kinetics and Pharmacology Distinct From Solvent-Based Paclitaxel

Nianhang Chen, PhD, Yan Li, PhD, Ying Ye, PhD, Maria Palmisano, MD, Rajesh Chopra, MD, PhD, and Simon Zhou, PhD

Abstract

The aim of this study was to characterize population pharmacokinetics and the exposure–neutropenia relationship with nanoparticle albumin-bound (*nab*)-paclitaxel in patients with solid tumors. Plasma and blood concentrations of paclitaxel and neutrophil data were collected from 150 patients with various solid tumors over the *nab*-paclitaxel dose range of 80–375 mg/m^2. Data were analyzed using nonlinear mixed-effect modeling or logistic regression. Pharmacokinetics of *nab*-paclitaxel were described by a 3-compartment model with saturable distribution and elimination. The rapid disappearance of circulating paclitaxel was driven by its fast distribution to peripheral compartments; maximum rate for saturable distribution (325000 μg/h) was 40-fold greater than that for saturable elimination (8070 μg/h). Albumin was a significant covariate of paclitaxel elimination ($P < .001$), while total bilirubin, creatinine clearance, body size, age, sex, and tumor type had no significant or clinically relevant effect. The probability of experiencing a ≥50% reduction in neutrophils was best correlated to the duration above the drug concentration of 720 ng/mL. At a given exposure level, neutropenia development was positively correlated with increasing age but not significantly influenced by hepatic function, tumor type, sex, or dosing schedule. Covariate analyses supports exposure-matched dose adjustments in patients with moderate to severe hepatic impairment.

Keywords

pharmacokinetics, pharmacodynamics, neutropenia, *nab*-paclitaxel, covariates

Nanoparticle albumin-bound (*nab*)-paclitaxel is a solvent-free, human albumin-stabilized formulation of paclitaxel.[1,2] *nab*-Paclitaxel was designed to improve the chemotherapeutic effects of paclitaxel and to reduce the toxicities, such as hypersensitivity reactions, associated with solvent-based (sb)-paclitaxel.[2] Because *nab*-paclitaxel is formulated with albumin, it exploits endogenous albumin transport pathways, resulting in enhanced transport across endothelial cell monolayers and greater delivery of paclitaxel to tumors, compared with sb-paclitaxel.[2] In phase III trials, *nab*-paclitaxel monotherapy demonstrated superior overall response rate versus sb-paclitaxel in metastatic breast cancer (MBC) and in combination with carboplatin in advanced non-small cell lung cancer (NSCLC).[3,4] In a recent phase III trial, *nab*-paclitaxel plus gemcitabine demonstrated a significant improvement in overall survival versus gemcitabine alone in patients with advanced pancreatic cancer,[5] a disease for which *nab*-paclitaxel is the only approved taxane for treatment.[1,6,7] Pharmacokinetics of *nab*-paclitaxel have previously been determined in clinical studies.[1,8] The systemic drug exposure was approximately proportional to *nab*-paclitaxel dose from 80 to 300 mg/m^2 and was independent of the intravenous infusion duration.[1,8] In contrast, sb-paclitaxel displays more than dose proportional increases in systemic drug exposure and infusion duration-dependent clearance over a narrower dose range,[9–12] likely due to entrapment of paclitaxel in micelles formed by the solvent Cremophor EL.[12,13] In a randomized crossover study of *nab*-paclitaxel 260 mg/m^2 infused over 30 minutes versus sb-paclitaxel 175 mg/m^2 infused over 3 hours, the fraction of unbound paclitaxel in plasma was 2.6-fold higher with *nab*-paclitaxel than with sb-paclitaxel.[14] Distribution and elimination kinetics and source of exposure variability have been described for sb-paclitaxel using population pharmacokinetic (PK) modeling,[15–17] but these data are currently not available for *nab*-paclitaxel.

Celgene Corporation, Summit, NJ, USA

Submitted for publication 23 January 2014; accepted 31 March 2014.

Corresponding Author:
Nianhang Chen, Celgene Corporation, Summit, NJ, USA
Email: nchen@celgene.com

Additionally, the relationship between sb-paclitaxel exposure and neutropenia, a common dose-limiting toxicity associated with taxane treatment, has been described using a threshold model.[10,18–21] In this model, the duration of paclitaxel plasma concentrations exceeding 0.05 μM was considered a strong predictor of neutropenia in patients with solid tumors. However, no such assessments have been performed for *nab*-paclitaxel. In randomized phase III trials involving patients with MBC or NSCLC, the incidence of severe neutropenia was significantly lower with *nab*-paclitaxel versus sb-paclitaxel despite delivery of a higher median cumulative dose of paclitaxel to patients receiving *nab*-paclitaxel versus sb-paclitaxel.[3,4]

Therefore, we conducted this study to establish a PK model that quantitatively describes the distribution and elimination of *nab*-paclitaxel and potential sources of interindividual PK variability, as well as to establish a pharmacodynamic (PD) model to quantitatively describe the relationship between *nab*-paclitaxel exposure and neutropenia.

Methods

Patient Population

Data from five phase I studies (including one study in patients with hepatic impairment),[8,14,22–24] one phase II study,[25] and two phase III studies[3,26] were included in this analysis (Supplemental Table S1). All patients had advanced or metastatic solid tumors. *nab*-Paclitaxel was administered as monotherapy in all studies and doses ranged from 80 to 375 mg/m^2, given on days 1, 8, and 15 of each 28-day cycle or day 1 of each 21-day cycle (every 3 weeks [q3w]). With the exception of one 135 mg/m^2 q3w dose cohort (infused over 3 hours), all doses were administered intravenously over 30 minutes. Whole blood (WB) or plasma samples were collected after the first dose. Paclitaxel concentrations were measured using validated high-performance liquid chromatography with tandem mass spectrometry[8,14,22,24]; lower limit of quantitation ranged from 1 to 10 ng/mL.

Population PK Model Development and Covariate Analysis

The population PK analysis was performed using the nonlinear mixed-effect modeling program (NONMEM version 7.2; ICON Development Solution, MD, US) with first-order conditional estimation with the INTERACTION (FOCEI) option. Paclitaxel concentration data were natural logarithm (Ln)-transformed. The model was built using both WB and plasma concentration data, and plasma PK parameters were estimated. An indicator was used to identify the matrix and a fixed-effect parameter of WB/plasma ratio was estimated to bridge WB and plasma concentrations for model fitting.

Saturable elimination was incorporated using the Michaelis–Menten equation and was described by the maximal elimination rate, VM_{EL}, and the drug concentration at which the elimination rate is half-maximal, KM_{EL}. Saturable distribution was incorporated analogous to the saturable elimination and was defined by the maximal distribution rate, VM_{TR}, and the concentration at which the distribution rate is half-maximal, KM_{TR}. Comparison of structural models was based on the objective function value (OFV). A value of $P < .001$, representing a decrease in OFV of greater than 10.83, was considered statistically significant (degrees of freedom (df) = 1). Interindividual variability (IIV) was modeled using an exponential error model. The assumption of a constant residue variability (RV) for all individuals from multi-center studies may result in biased variable estimates. To reduce this possible bias, RV was modeled with two subpopulations using a proportional error model and the MIXEST function in NONMEM.

Candidate covariates tested during PK model building included age, body weight, body surface area (BSA), sex, race, total bilirubin, albumin, creatinine clearance (CrCl, estimated by Cockcroft-Gault formula), and tumor type. Covariates were initially selected by graphic inspection and biological plausibility. Further testing of potential covariates was performed by univariate analysis, stepwise forward addition ($P < .01$) and backward elimination ($P < .001$) based on changes in OFV and inspection of model diagnostic plots. Continuous covariates were centered to their median values and included as power models. Categorical covariates were included as discrete indicator variables. Multiplicative equations were used to describe and test the combined effect of multiple covariates on the same parameter.

Stability of the final PK parameter estimates and 95% CIs were evaluated using the non-parametric bootstrap approach and the ability of the final population PK model to describe observed concentration data was evaluated by visual predictive checks (VPC).

Population PD Model Development and Covariate Analysis

The analysis population included patients who had paclitaxel concentration and evaluable absolute neutrophil count (ANC) data in the first treatment cycle. Patients suspected of growth factor use were excluded. The population PD analysis was performed using NONMEM with the FOCEI option. Empiric individual Bayesian estimates of paclitaxel PK parameters obtained from the final population PK model were used as input variables to estimate drug concentrations in plasma for PD modeling. The time course of circulating ANC was characterized by an 8-compartment semimechanistic population PK/PD model: a 3-compartment PK model and a 5-compartment PD model for neutropenia (Figure 1) as proposed by

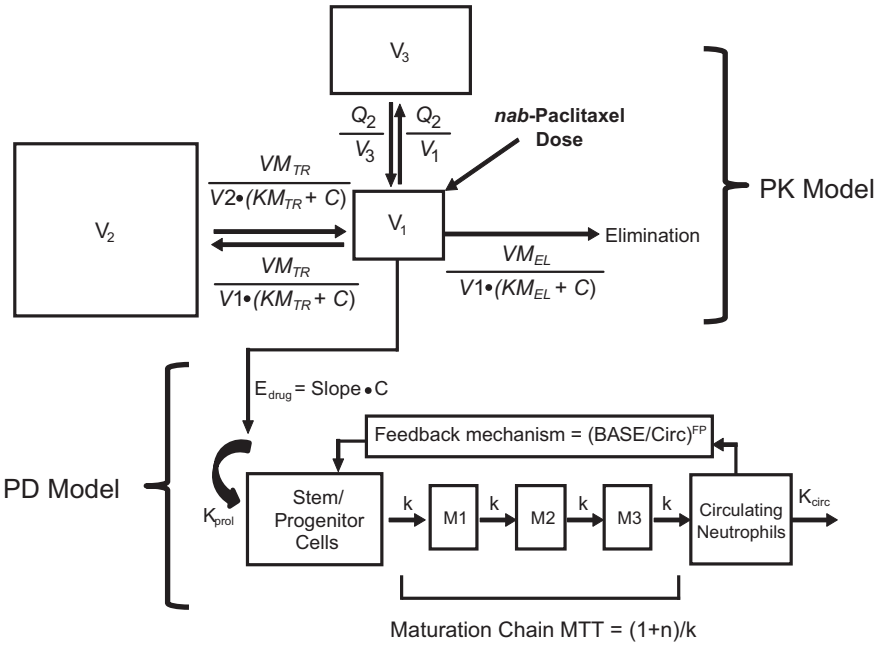

Figure 1. Structure of the final population pharmacokinetic/pharmacodynamic model. This model describes the systemic paclitaxel concentration–time profile and circulating neutrophil–time profile. BASE, baseline neutrophil counts; C, paclitaxel concentration; Circ, circulating neutrophil counts; E_{drug}, drug effect; FP, feedback parameter; k, intercompartmental transfer rate constant; k_{circ}, elimination rate constant; k_{prol}, proliferation rate constant; KM_{EL}, paclitaxel concentration in the central compartment at 50% of VM_{EL}; KM_{TR}, paclitaxel concentration in the central compartment at 50% of VM_{TR}; M1, maturation compartment 1; M2, maturation compartment 2; M3, maturation compartment 3; MTT, mean transit time; n, number of maturation compartments; PD, pharmacodynamic; PK, pharmacokinetic; Q_2, intercompartmental clearance between the central compartment and the second peripheral compartment; V_1, volume of distribution for the central peripheral compartment; V_2, volume of distribution for the first peripheral compartment; V_3, volume of distribution for the second peripheral compartment; VM_{EL}, maximum elimination rate from the central compartment; VM_{TR}, maximum intercompartmental distribution rate between the central compartment and the first peripheral compartment.

Friberg et al.[17] The PD model was based on the maturation process of neutrophil precursor cells and consisted of a compartment for stem/progenitor cells, three compartments for cell maturation, and one compartment for circulating ANC. From the PD model, time delay between drug exposure, impaired cell proliferation, and the resulting effect on circulating ANC could be described.

Parameter estimates for the PD model included the drug effect Slope, a linear proportionality constant relating paclitaxel concentration in the central compartment to its effect on bone marrow stem or progenitor cells; a feedback parameter that quantifies the strength of feedback action from release of endogenous growth factors as a response to decreased cells in the circulation pools, which was dependent on the ratio of baseline ANC and levels of ANC in circulation; and mean transit time (MTT), the average time for a stem cell to pass through the three compartments for cell maturation in the bone marrow before it is released into the circulation. MTT was derived by the following equation: $MTT = (n + 1)/k$ where n was the number of maturation compartments ($n = 3$) and k was the intercompartmental transfer rate constant.

ANC values were Ln-transformed. IIV was modeled using an exponential error model. RV was modeled using a proportional error model. Age, sex, dosing schedule, type of tumor, total bilirubin, and albumin were tested as possible covariates of PD parameters. Selection of covariates for the PD portion followed similar procedures and statistical criteria as described for the population PK analysis.

The ability of the final PD model to describe observed ANC data was evaluated by performing VPC and numeric predictive checks.

Logistic Regression Model, Threshold Analysis, and Covariate Analysis

Logistic regression analyses were conducted using S-PLUS to describe the relationship between systemic paclitaxel exposure and probability of the event (a $\geq$50% reduction in ANC). The probability that the event occurred as a function of independent variables was described as follows:

$$\mathrm{Ln\,(odds)} = \mathrm{Ln}\left(\frac{P_i}{1 - P_i}\right) = \alpha + \beta_1 X_1 + \beta_2 X_2 + \ldots \beta_n X_n$$

where P_i is the probability of the event in the "i"th patient and α is the baseline Ln (odds) of the event. The $\beta_1 \ldots \beta_n$

is adjusted odds ratio [OR] characterizing the dependence of the Ln (odds) on 1 or more covariates, $X_1 \ldots X_n$. Paclitaxel exposure, age, BSA, sex, race, dosing schedule, type of tumor, total bilirubin, albumin, and baseline ANC were examined as covariates in univariate and multivariate logistic regression analyses.

The paclitaxel exposure measures were the population PK model-predicted area under the concentration–time curve (AUC), maximum concentration (C_{max}), and the duration above a certain concentration level.

A threshold analysis was conducted to explore whether there was a paclitaxel concentration level above which correlated with the event. Briefly, the cumulative duration above a threshold concentration during the first treatment cycle was computed based on ≈100 concentration cutoff values, ranging from 1 to 1000 ng/mL with an increment of 10 ng/mL for each patient. Univariate logistic regression was performed for the duration above each concentration cutoff level to test the statistical significance in predicting the probability of experiencing a ≥50% reduction in ANC.

Results

Population PK Model

Analysis population. A total of 1418 evaluable paclitaxel concentration records from 150 patients were included in the final population PK model. Baseline characteristics are summarized in Table 1. Median total bilirubin was 8.6 μM with 13.3% of patients having a value above the upper limit of normal (ULN) of 17 μM and 8% of patients having moderate to severe hepatic impairment (total bilirubin >1.5 to ≤5 ULN). Median CrCl for the patient population was 82.7 mL/min with 15.3% patients having moderate renal impairment (CrCl 30 to <60 mL/min).

Structural model characteristics. With a higher than dose-proportional increase in exposure observed at the highest dose level (375 mg/m^2), a 3-compartment PK model with saturable elimination was preferred over a linear elimination model ($\Delta OFV = -502$, $P < .0001$). Subsequently, a saturable distribution model was preferred over a first-order distribution model (ΔOFV: −141, $P < .0001$). Using two subgroups with separate RV was superior to adopting a single RV for the whole analysis population (ΔOFV: −134, $P < .0001$). Thus, a 3-compartment PK model with saturable elimination from the central compartment, saturable distribution between the central compartment and first peripheral compartment, and first-order distribution between the central compartment and second peripheral compartment was selected as the final structural PK model. Shrinkage associated with VM_{EL} and volume of distribution for the central peripheral compartment (V_1) was 22.1% and 24.4%, respectively, and covariate analysis was conducted subsequently for the two parameters.

Covariate analysis. The covariate analysis revealed a significant ($P < .001$) correlation between baseline albumin level and VM_{EL} as expressed in the following equation:

$$VM_{EL} = 8070 \times (\text{albumin}/3.9)^{0.554}$$

The model suggested that VM_{EL} decreased with decreasing albumin level, with an ≈30% reduction in VM_{EL} at the albumin level of 2 g/dL. Although the effect of albumin on VM_{EL} was statistically significant, the contribution of albumin to the overall IIV of VM_{EL} was marginal, reducing it from 23.6% in the structural model to 22.3% in the final model. No other significant correlations were observed between candidate covariates and VM_{EL} or V_1 in covariate modeling.

Table 1. Demographic and Baseline Characteristics of the Pharmacokinetic and Pharmacodynamic Patient Populations

Variable	Pharmacokinetic, N = 150	Pharmacodynamic, N = 125
Median age (range), year	57 (24–85)	56 (24–83)
Female, n (%)	90 (60)	79 (63)
Race, n (%)		
White	136 (91)	114 (91)
Asian	13 (9)	10 (8)
Black	1 (<1)	1 (<1)
Tumor type, n (%)		
Breast cancer	24 (16)	20 (16)
Melanoma	44 (29)	40 (32)
Other solid tumors	82 (55)	65 (52)
Body weight, median (range), kg	74 (40–143)	73 (40–143)
Body surface area, median (range), m^2	1.9 (1.3–2.4)	1.8 (1.3–2.4)
Albumin, median (range), g/dL	3.9 (2.1–4.7)	4.0 (2.1–4.7)
Total bilirubin, median (range), μM	8.6 (3.4–81.0)	8.6 (3.4–81.0)
Alkaline phosphatase, median (range), U/L	94 (42–2003)	94 (42–2003)
Creatinine clearance, median (range), mL/min	82.7 (29.6–150.0)	82.3 (42.3–150.0)

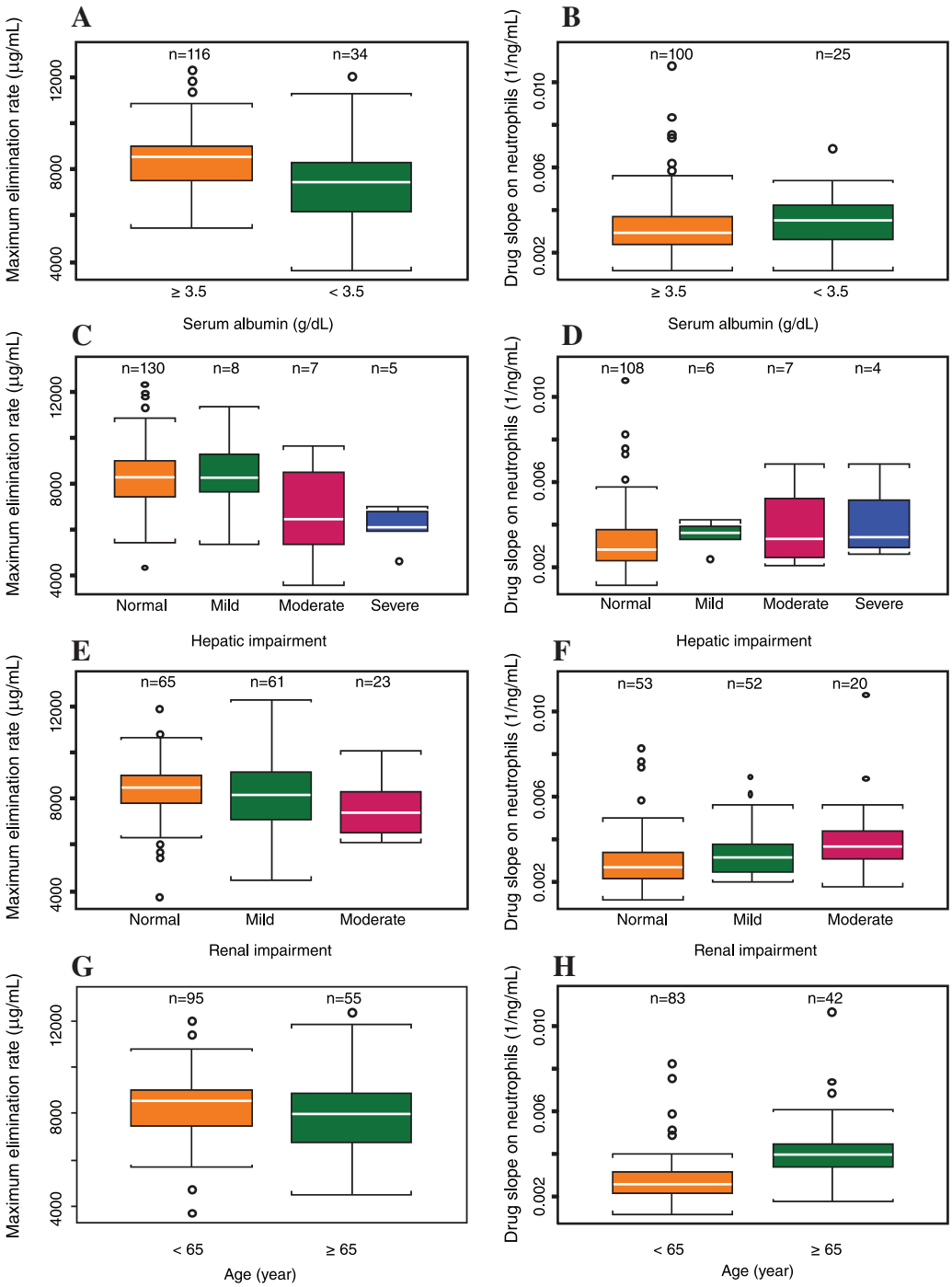

Figure 2. Effect of albumin, hepatic impairment, renal impairment, and age on the maximum elimination rate of *nab*-paclitaxel (left panels A, C, E, and G) and the neutrophil inhibition by *nab*-paclitaxel (right panels B, D, F, and H). The white line in each boxplot represents the median value. The height of each of the box corresponds to the interval between the first and the third quartiles. The first bar (adjacent value) on either side of the box joined by a line expand the interval to 1.5 times the interquartile range, and the single points beyond the adjacent value are the outside values. In panels C and D, the total bilirubin values at baseline were used to categorize patients into different hepatic function groups according to the National Cancer Institute Organ Dysfunction Working Group criteria[27]: normal hepatic function (total bilirubin $\leq 1 \times$ ULN), mild hepatic impairment (total bilirubin >1 to $\leq 1.5 \times$ ULN), moderate hepatic impairment (total bilirubin >1.5 to $\leq 3 \times$ ULN), and severe hepatic impairment (total bilirubin >3 to $\leq 5 \times$ ULN). In panels E and F, the CrCl value at baseline were used to categorize patients into different renal function groups: normal renal function (CrCl ≥ 90 mL/min), mild renal impairment (CrCl 60 to <90 mL/min), and moderate renal impairment (CrCl 30 to <60 mL/min). CrCl, creatinine clearance; ULN, upper limit of normal.

Table 2. Final Population PK and PD Parameters of Paclitaxel When Administered as *nab*-Paclitaxel

	Unit	Estimate	95% CI[a,b]	RSE,[b] %
PK parameter				
V_1	L	15.8	13.71–17.85	6.20
V_2	L	1650	1396–1935	7.9
V_3	L	75.4	59.8–99.1	11.7
VM_{TR}	μg/h	325000	190694–540445	25.8
KM_{TR}	μg/L	4260	2210–7910	33.1
Q_2	L/h	41.6	35.1–50.0	8.5
VM_{EL}	μg/h	8070	6500–9836	10.1
KM_{EL}	μg/L	40.2	24.9–58.9	20.0
WB/PL ratio		1.00	0.93–1.10	4.3
Fraction of subpopulation 1		0.341	0.20–0.53	24.5
Albumin on VM_{EL}		0.554	0.15–0.94	37.5
Interindividual variability				
V_1	%	46.7	29.5–63.4	33.1
V_2	%	25.5	18.2–39.7	40.9
VM_{TR}	%	26.7	18.7–35.5	28.6
VM_{EL}	%	22.3	17.1–27.4	22.4
WB/PL ratio	%	16.7	8.1–23.4	36.9
Residual variability				
Subpopulation 1	%	38.0	31.8–46.9	17.1
Subpopulation 2	%	17.9	15.1–19.7	17.8
PD parameter				
MTT	h	117	109–125	3.4
Drug slope	1/ng/mL	0.00253	0.00216–0.00290	7.47
Baseline ANC	10^9/L	4.28	3.94–4.62	4.09
Feedback parameter		0.187	0.171–0.203	4.44
Age on drug slope		0.501	0.172–0.830	33.5
Albumin on baseline ANC		−0.998	−1.5 to −0.494	25.8
Interindividual variability				
MTT	%	19.0	12.9–23.6	27.5
Slope	%	42.9	32.1–51.5	22.3
Baseline ANC	%	35.1	28.2–40.9	18.0
Residual variability	%	29.1	24.0–33.3	16.1

ANC, absolute neutrophil count; KM_{EL}, paclitaxel concentration in the central compartment at 50% of VM_{EL}; KM_{TR}, paclitaxel concentration in the central compartment at 50% of VM_{TR}; MTT, mean transit time; PD, pharmacodynamic; PK, pharmacokinetic; PL, plasma; Q_2, intercompartmental clearance between the central compartment and the second peripheral compartment; RSE, relative standard error; V_1, volume of distribution for the central peripheral compartment; V_2, volume of distribution for the first peripheral compartment; V_3, volume of distribution for the second peripheral compartment; VM_{EL}, maximum elimination rate from the central compartment; VM_{TR}, maximum intercompartmental distribution rate between the central compartment and the first peripheral compartment; WB, whole blood.

[a]95% CI and RSE% for the PK parameter estimates were obtained from the nonparametric bootstrap resampling procedure.

[b]95% CI and RSE% for the PD parameter estimates were obtained from NONMEM.

Effect of albumin, total bilirubin, CrCl, and age on paclitaxel elimination was further examined by categorical analysis of individual estimates of VM_{EL} from the final PK model (Figure 2A, 2C, 2E, and 2G). Median VM_{EL} in patients with albumin below the lower limit of normal (<3.5 g/dL) was reduced by 12%, compared with patients with normal albumin levels (Figure 2A). The total bilirubin values at baseline were used to categorize patients into different hepatic function groups. Median VM_{EL} appeared similar among patients with mild hepatic impairment and those with normal hepatic function (Figure 2C). Median VM_{EL} in patients with moderate or severe hepatic impairment was reduced by 22% or 26%, respectively, compared with patients with normal hepatic function (Figure 2C). The CrCl values at baseline were used to categorize patients into different renal function groups. Median VM_{EL} between patients with mild or moderate renal impairment was similar to that of patients with normal renal function (Figure 2E). In addition, no apparent difference in VM_{EL} was observed between age groups (Figure 2G).

Final PK model and model evaluation. Final population PK parameter estimates are reported in Table 2. The IIV was determined for V_1, V_2, VM_{TR}, VM_{EL}, and WB/plasma ratio. Inclusion of IIV for the other PK parameters did not improve the fit, indicating that the data contained

insufficient information to estimate these variables. There was no obvious bias in the prediction of paclitaxel concentrations at the population and individual levels or at a specific time point (Supplemental Figure S1). Relative differences between the final model estimates and median values of the parameters obtained from bootstrap replications (500 runs with 95% minimized) were $\leq$15% for the fixed-effect parameters and $\leq$4% for the random-effect parameters. In VPC evaluation, the 5th, 50th, and 95th percentiles of the observed concentration data at each time point were generally within the respective 95% CI of the simulated data suggesting that the final model was robust and stable.

Population PD Model of Neutropenia

Analysis population. A total of 558 ANC data records collected from 125 patients during the first treatment cycle were included in the final analysis data set. Baseline characteristics of patients included in the model were similar to those for the population PK analysis (Table 1). Approximately 9% of patients had moderate to severe hepatic impairment and ≈16% of patients had moderate renal impairment. During the first treatment cycle, 48.8% of patients received three doses of *nab*-paclitaxel weekly and 51.2% of patients received one dose q3w. The median ANC at baseline was 4.45×10^9/L (range, 1.7–15×10^9/L).

Covariate analysis. Shrinkage associated with baseline ANC and Slope in the structural model was 11.6% and 24.6%, respectively, and a covariate analysis was conducted subsequently for the two parameters.

Effect of age on Slope was modeled both as a continuous variable and as a dichotomized variable (<65 years vs. ≥65 years). The later approach had a greater statistical significance ($\Delta OFV = -12.8$ vs. $\Delta OFV = -9.9$) and is also consistent with clinical practice. Thus, it was incorporated into the final model as follows:

$$\text{Paclitaxel effect slope} = 0.00253 \ (1.501 \text{ for age} \geq 65 \text{ years})$$

The typical value for paclitaxel effect slope was 0.00253 for patients aged <65 years and 0.0038 for patients aged ≥65 years, indicative of a decrease in the proliferation rate of 25% and 38% per 100 ng/mL paclitaxel plasma concentration, respectively. The model suggested an increased susceptibility (+50%) to the inhibitory effect of paclitaxel on neutrophil precursor proliferation in elderly patients (Figure 2H). Although the effect of age on paclitaxel effect slope was statistically significant, the contribution of age to the IIV was marginal, reducing IIV from 45.5% in the base model to 42.9% in the final model.

Inclusion of albumin as a covariate of baseline ANC improved the goodness-of-fit of the model ($P < .001$). However, the physiological and clinical relevance of the baseline ANC–albumin correlation is unclear. No other significant correlations were observed between candidate covariates and Slope or baseline ANC in the covariate analysis.

Effect of albumin, hepatic impairment, renal impairment, and age on drug effect was further examined by categorical analysis of individual estimates of Slope from the final PD model (Figure 2B, 2D, 2F, and 2H). Median Slope appeared similar in patients with mild or moderate to severe hepatic impairment and those with normal hepatic function (Figure 2D). No apparent differences in Slope were observed across renal function categories (Figure 2F) when age difference was considered (more elderly patients in the moderate renal impairment group).

Final PD model and model evaluation. PD parameter estimates from the final model are shown in Table 2. All parameters were estimated with good precision (RSE $\leq$ 35%). IIV for Slope was high (42.9%), and similar to that reported for other oncology drugs.[17] Estimates of the systemic parameters, including MTT, feedback parameter, and baseline ANC, were also similar to those reported for other oncology drugs.[17] There was no obvious bias in the prediction of ANCs at the population and individual levels or at a specific time point (Supplemental Figure S2). For the 260 mg/m^2 q3w *nab*-paclitaxel dosing regimen, observed and predicted ANC nadir occurred at ≈1 week versus 2 weeks for the 150 mg/m^2 weekly regimen. Observed and predicted ANC returned to baseline values at ≈3 and 4 weeks, respectively.

Model evaluation with VPC suggested that the final model adequately characterized the central tendency and variability of ANC versus time profiles from the 5th to 95th percentiles for each dosing schedule. The observed percentages of patients who experienced grade ≥3 neutropenia were 21.3% for weekly dosing and 23.4% for q3w dosing and they were well contained within the 95% CIs for the percentages obtained from the numeric predictive check (Supplemental Figure S3), supporting model adequacy.

Logistical Regression and Threshold Analysis for Neutropenia

In the univariate threshold analysis, the minimum *P*-value was observed for duration (Figure 3A) and AUC (Figure 3B) above the concentration 720 ng/mL. Thus, paclitaxel exposure above 720 ng/mL was best correlated with the probability of experiencing a ≥50% reduction in ANC during the first cycle of treatment.

Although more-sensitive exposure metrics were available (eg, AUC above 720 ng/mL), only C_{max} and AUC were tested as the exposure measure in the multivariate analysis due to practical consideration. Both C_{max} and AUC were significant predictors. The adjusted OR for Ln(C_{max}) and Ln(AUC) was 2.369 (95% CI, 1.189–4.719; $P = .014$) and 2.228 (95% CI, 1.109–

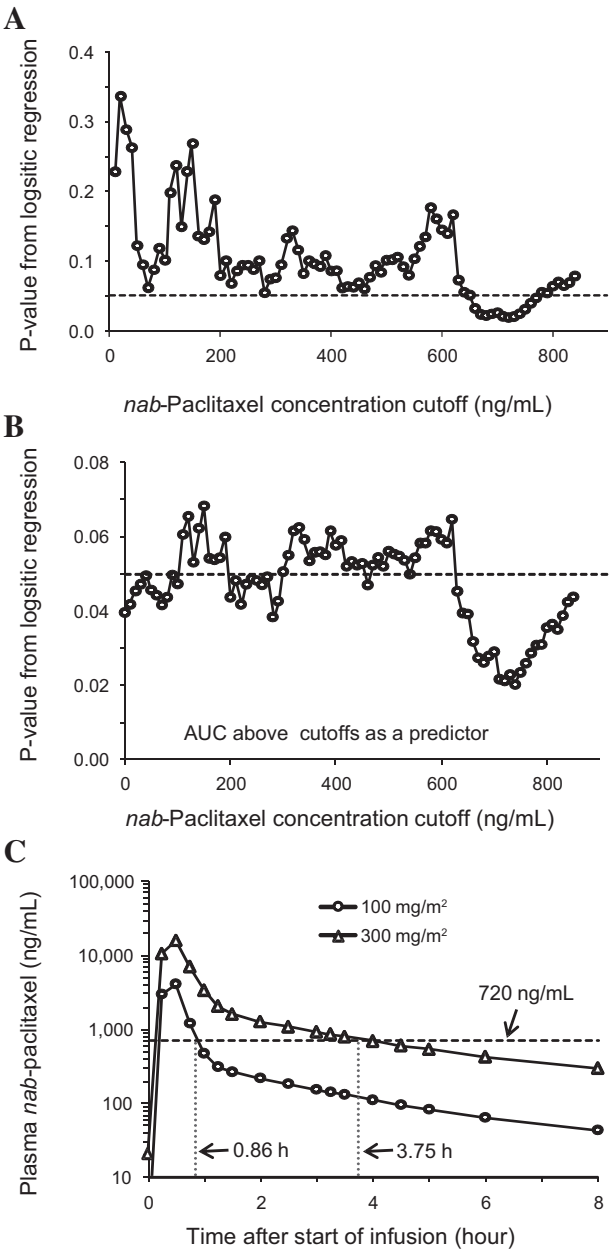

Figure 3. Statistical comparison of different threshold concentrations as the predictor of probability of experiencing a ≥50% reduction in absolute neutrophil counts and simulated concentration profiles. In panels A and B, each point represents the *P*-value corresponding to the time (A) or AUC (B) above a particular cutoff value of *nab*-paclitaxel concentration; the horizontal dashed line represents a *P*-value of .05. In panel C, points represent the simulated paclitaxel concentrations at the *nab*-paclitaxel dose of 100 and 300 mg/m^2 (given as a 30-minute IV infusion), respectively; the horizontal dash line represents the threshold concentration of 720 ng/mL. The duration above 720 ng/mL is indicated for each dose level. AUC, area under the concentration–time curve; IV, intravenous.

4.475; $P = .024$), respectively. This suggests that 1 logarithmic increase in C_{max} or AUC has a multiplicative effect of 2.369 or 2.228 on the odds of having a 50% reduction in ANC. Age was also a significant predictor of ANC reduction (OR 1.030; $P < .05$), regardless of which exposure measure (C_{max} or AUC) was included in the multivariate analysis. Hepatic impairment, renal impairment, type of solid tumor, sex, and dosing schedule were not predictive of neutropenia in the logistical regression analysis.

Table 3. Comparison of the Main Population PK and PD parameters Between *nab*-Paclitaxel and sb-Paclitaxel

	Unit	*nab*-Paclitaxel	sb-Paclitaxel
PK parameter[a]			
V_1	L	15.8	12.8
V_2	L	1650	177[b]
V_3	L	75.4	252
VM_{TR}	μg/h	325000	144326
KM_{TR}	μg/L	4260	708
Q_2	L/h	41.6	20.1
VM_{EL}	μg/h	8070	31931
KM_{EL}	μg/L	40.2	452
PD parameter[c]			
MTT	h	117	127
Slope[d]	1/ng/mL	0.0025	0.0026
Baseline ANC	10^9/L	4.28	5.2
Feedback parameter		0.19	0.23

ANC, absolute neutrophil count; KM_{EL}, paclitaxel concentration in the central compartment at 50% of VM_{EL}; KM_{TR}, paclitaxel concentration in the central compartment at 50% of VM_{TR}; MTT, mean transit time; PD, pharmacodynamic; PK, pharmacokinetic; PL, plasma; Q_2, intercompartmental clearance between the central compartment and the second peripheral compartment; sb, solvent-based; V_1, volume of distribution for the central peripheral compartment; V_2, volume of distribution for the first peripheral compartment; V_3, volume of distribution for the second peripheral compartment; VM_{EL}, maximum elimination rate from the central compartment; VM_{TR}, maximum intercompartmental distribution rate between the central compartment and the first peripheral compartment; WB, whole blood.

[a]Reference values for sb-paclitaxel were reported by Joerger et al.[15]

[b]The value is derived from the original parameters reported by Joerger et al with the assumption that the drug concentration in the first peripheral compartment is far below the KM_{TR} (ie, the highest possible volume).

[c]Reference values for sb-paclitaxel were reported by Friberg et al.[17]

[d]Slopes for both *nab*-paclitaxel and sb-paclitaxel correspond to total drug.

Discussion

This is the first-reported meta-analysis of the population pharmacokinetics and exposure–neutropenia relationship for *nab*-paclitaxel. Because the models described here were structurally identical to those previously described for sb-paclitaxel, we were able to identify distinct PK and similar PD features of the two paclitaxel formulations (Table 3).[15,17] *nab*-Paclitaxel had a significant effect on the distribution and elimination kinetics of paclitaxel without altering the intrinsic cytotoxic effect of paclitaxel on neutrophils.

Concentration–time data of paclitaxel administered as *nab*-paclitaxel over a dose range from 80 to 375 mg/m^2 to

patients with solid tumors were adequately described by a 3-compartment model with saturable elimination from the central compartment and saturable distribution to the first peripheral compartment. The rapid disappearance of paclitaxel from circulation was primarily driven by its fast distribution from the central compartment to peripheral compartments as demonstrated by the 40-fold greater maximal rate of saturable tissue distribution (325000 μg/h) compared to the maximal rate of saturable elimination (8070 μg/h) from the central compartment. The distribution of paclitaxel to tissues was not only rapid, but also extensive, with deep tissue penetration as demonstrated by the finding that the volume of the two peripheral compartments (75 and 1650 L) far exceeded the total body water volume (≈40 L).

Comparison of this analysis to the PK analysis previously described for sb-paclitaxel shows that the population paclitaxel PK parameters for *nab*-paclitaxel are markedly different (Table 3).[15] The rates of the first-order distribution and saturable distribution of paclitaxel more than doubled when administered as *nab*-paclitaxel versus sb-paclitaxel, suggesting faster drug distribution into tissues with *nab*-paclitaxel. The distribution volume of the peripheral compartment involving saturable distribution was ≈9-fold larger when administered as *nab*-paclitaxel (1650 L) versus sb-paclitaxel (177 L), suggesting deeper penetration of the drug into tissues via transporter-mediated pathways with *nab*-paclitaxel. While distribution of paclitaxel was clearly much faster and deeper following administration of *nab*-paclitaxel, elimination of paclitaxel was much slower with *nab*-paclitaxel versus sb-paclitaxel. This was demonstrated by smaller VM_{EL} (8070 μg/h vs. 31931 μg/h) and KM_{EL} (40.2 μg/L vs. 452 μg/L) values. Such changes may explain why *nab*-paclitaxel allows for dose-proportional increases in the systemic exposure of paclitaxel over a broader dose range than does sb-paclitaxel (ie, the majority of circulating-drug AUC is governed by distribution, rather than elimination, and the saturable distribution has a larger capacity).[1,8–12]

The paclitaxel concentration ratio of whole blood to plasma was estimated to be 1.0, indicating that paclitaxel was evenly distributed between cellular and plasma components of whole blood when administered as *nab*-paclitaxel. This observation is consistent with the improved distribution property of paclitaxel when administered as *nab*-paclitaxel. In contrast, after administration of sb-paclitaxel, a large amount of paclitaxel remains in the plasma and is not readily distributed to blood cells.[28]

Because paclitaxel is eliminated by hepatic metabolism and biliary excretion, two indicators of hepatic impairment—albumin (produced in the liver) and total bilirubin (metabolized in the liver and excreted into bile)—were evaluated for their ability to predict paclitaxel elimination. In the covariate analysis, changes in either serum albumin or total bilirubin had limited effect on paclitaxel elimination when administered as *nab*-paclitaxel. In a previous study in patients with hepatic impairment who were treated with *nab*-paclitaxel, total bilirubin levels were inversely correlated to paclitaxel clearance.[24] However, that study had no patients with normal hepatic function for PK comparison. The present analysis included both patients with hepatic impairment[24] and patients with normal hepatic function (Supplemental Table S1). With a larger data set and considering IIV in patients, a negative trend between VM_{EL} and total bilirubin did not reach significance in the covariate analysis. The mean reduction in VM_{EL} was estimated to be 26% in patients with total bilirubin >3 to $\leq 5\times$ ULN compared with patients with a normal total bilirubin level. In contrast, when paclitaxel is administered as sb-paclitaxel, it appears that total bilirubin is a more sensitive predictor of paclitaxel elimination.[15] Paclitaxel elimination was also significantly influenced by age, sex, and BSA when administered as sb-paclitaxel.[15] However, these factors did not appear to influence paclitaxel elimination when administered as *nab*-paclitaxel.

The total drug concentration was selected over the free drug concentration in exposure–response analysis for *nab*-paclitaxel, as (1) the albumin-bound form of paclitaxel likely contributes to its pharmacology, and (2) the fraction of free drug in plasma is constant over the clinical ranges of total drug concentrations (data not shown). The neutropenia model showed a similar inhibitory potency (Slope) on ANC between *nab*-paclitaxel and sb-paclitaxel (Table 3), suggesting a lack of differences in the intrinsic effect of paclitaxel on ANC.[16] Therefore, the differences observed in neutropenia frequency in the phase III trials[3,4] was more likely driven by the different concentration profiles between the two formulations. The threshold analysis for *nab*-paclitaxel showed that the probability of experiencing a $\geq$50% reduction in ANC was best correlated to the duration above the paclitaxel concentration of 720 ng/mL (0.84 μM). In contrast, the duration above a low threshold paclitaxel concentration of 0.05 or 0.1 μM, as previously reported for sb-paclitaxel,[10,29] was not significantly correlated. These concentrations were too low to differentiate interindividual difference. The more rapid distribution of paclitaxel into tissues when administered as *nab*-paclitaxel results in shorter duration of high drug systemic concentrations, which likely contributes to the less frequent severe neutropenia observed with *nab*-paclitaxel versus sb-paclitaxel in the phase III MBC and NSCLC trials.[3,4] The threshold analysis results also provide insight into *nab*-paclitaxel dosing regimens. A reduced frequency of severe neutropenia (25% vs. 44%) but similar efficacy was reported for weekly dosing (100 mg/m^2) versus q3w dosing (300 mg/m^2) of *nab*-paclitaxel in patients with breast cancer.[30] Under these

conditions, the simulated duration above 720 ng/mL per cycle was reduced by 31% for weekly dosing versus q3w dosing (Figure 3C).

Our analysis with *nab*-paclitaxel demonstrated that risk of neutropenia is positively correlated with increasing age, consistent with observations from other chemotherapies.[28] Elderly patients are more likely to have reduced bone marrow reserve and hence more susceptible to myelosuppression with therapeutic doses of cytotoxic drugs. This may explain the increased drug effect Slope in elderly patients (+50%) in the final neutropenia model. Additionally, our findings that hepatic impairment was not a significant predictor of neutropenia after adjusting for the systemic exposure of paclitaxel is consistent with the previous findings of the hepatic impairment study with *nab*-paclitaxel, in which ANC was correlated with paclitaxel exposure but not total bilirubin.[24] However, our observation with *nab*-paclitaxel was different from that reported for sb-paclitaxel which demonstrated that patients with high total bilirubin appeared more susceptible to neutropenia even at a reduced systemic exposure of paclitaxel.[31]

Because the effect of hepatic impairment on paclitaxel elimination and neutropenia is different from that reported for sb-paclitaxel, simple extrapolation of the hepatic dosages from sb-paclitaxel to *nab*-paclitaxel is not supported. A reduction of ≈20% in the starting *nab*-paclitaxel dose may be considered for patients with total bilirubin > 1.5 to $\leq 5 \times$ ULN to avoid a potential increase in systemic drug exposure. A larger reduction in the *nab*-paclitaxel starting dose for these patients may not be warranted based on the following observations: (1) the modest reduction in drug elimination at high total bilirubin levels (up to 26%, translated into an ≈20% mean increase in AUC based on simulations); (2) the limited contribution (<2%) of hepatic impairment to the IIV of drug elimination (systemic exposure); and (3) the lack of correlation of total bilirubin to neutropenia. In addition, extensive dose reduction may lead to under treatment of patients. This analysis does not include pancreatic cancer patients with mechanic obstruction of the bile duct, and the *nab*-paclitaxel dose in this special population remains to be elucidated in future studies. The present analysis also suggested that a reduction in the starting *nab*-paclitaxel dose is not necessary for patients with mild to moderate renal impairment, as CrCl ($\geq$30 mL/min) was not a significant predictor of either drug elimination or neutropenia.

In summary, *nab*-paclitaxel causes more rapid and deeper tissue penetration and slower elimination of paclitaxel compared with sb-paclitaxel. Less-frequent neutropenia with *nab*-paclitaxel can be explained by the rapid decline of paclitaxel concentrations below the threshold of 720 ng/mL in circulation. The covariate analysis supports exposure-matched dose adjustments in patients with hepatic impairment and suggests that no dose adjustments are needed in patients with mild to moderate renal impairment. The results reveal important pharmacologic features of *nab*-paclitaxel distinct from sb-paclitaxel, which likely contribute to the differences in clinical safety and efficacy between the two formulations.

References

1. Abraxane [package insert]. Summit, NJ: Celgene Corporation; 2013.
2. Desai N, Trieu V, Yao Z, et al. Increased antitumor activity, intratumor paclitaxel concentrations, and endothelial cell transport of Cremophor-free, albumin-bound paclitaxel, ABI-007, compared with Cremophor-based paclitaxel. *Clin Cancer Res*. 2006; 12(4):1317–1324.
3. Gradishar WJ, Tjulandin S, Davidson N, et al. Phase III trial of nanoparticle albumin-bound paclitaxel compared with polyethylated castor oil-based paclitaxel in women with breast cancer. *J Clin Oncol*. 2005;23(31):7794–7803.
4. Socinski MA, Bondarenko I, Karaseva NA, et al. Weekly *nab*-paclitaxel in combination with carboplatin versus solvent-based paclitaxel plus carboplatin as first-line therapy in patients with advanced non-small-cell lung cancer: final results of a phase III trial. *J Clin Oncol*. 2012;30(17):2055–2062.
5. Von Hoff DD, Ervin TJ, Arena FP, et al. Increased survival in pancreatic cancer with nab-paclitaxel plus gemcitabine. *N Engl J Med*. 2013;369(18):1691–1703.
6. Taxol [package insert]. Princeton, NJ: Bristol-Meyers Squibb Company; 2011.
7. Taxotere [package insert]. Bridgewater, NJ: sanofi-aventis U.S. LLC; 2013.
8. Ibrahim NK, Desai N, Legha S, et al. Phase I and pharmacokinetic study of ABI-007, a Cremophor-free, protein-stabilized, nanoparticle formulation of paclitaxel. *Clin Cancer Res*. 2002;8(5):1038–1044.
9. Sonnichsen DS, Hurwitz CA, Pratt CB, Shuster JJ, Relling MV. Saturable pharmacokinetics and paclitaxel pharmacodynamics in children with solid tumors. *J Clin Oncol*. 1994;12(3):532–538.
10. Gianni L, Kearns CM, Giani A, et al. Nonlinear pharmacokinetics and metabolism of paclitaxel and its pharmacokinetic/pharmacodynamic relationships in humans. *J Clin Oncol*. 1995;13(1):180–190.
11. van Tellingen O, Huizing MT, Panday VR, Schellens JH, Nooijen WJ, Beijnen JH. Cremophor EL causes (pseudo-) non-linear pharmacokinetics of paclitaxel in patients. *Br J Cancer*. 1999;81-(2):330–335.
12. Sparreboom A, van Tellingen O, Nooijen WJ, Beijnen JH. Nonlinear pharmacokinetics of paclitaxel in mice results from the pharmaceutical vehicle Cremophor EL. *Cancer Res*. 1996; 56(9):2112–2115.
13. Sparreboom A, van Zuylen L, Brouwer E, et al. Cremophor EL-mediated alteration of paclitaxel distribution in human blood: clinical pharmacokinetic implications. *Cancer Res*. 1999; 59(7):1454–1457.
14. Gardner ER, Dahut WL, Scripture CD, et al. Randomized crossover pharmacokinetic study of solvent-based paclitaxel and *nab*-paclitaxel. *Clin Cancer Res*. 2008;14(13):4200–4205.
15. Joerger M, Huitema AD, van den Bongard DH, Schellens JH, Beijnen JH. Quantitative effect of gender, age, liver function, and body size on the population pharmacokinetics of paclitaxel in patients with solid tumors. *Clin Cancer Res*. 2006;12(7 pt 1):2150–2157.

16. Joerger M, Huitema AD, Richel DJ, et al. Population pharmacokinetics and pharmacodynamics of paclitaxel and carboplatin in ovarian cancer patients: a study by the European Organization for Research and Treatment of Cancer-Pharmacology and Molecular Mechanisms Group and New Drug Development Group. *Clin Cancer Res*. 2007;13(21):6410–6418.
17. Friberg LE, Henningsson A, Maas H, Nguyen L, Karlsson MO. Model of chemotherapy-induced myelosuppression with parameter consistency across drugs. *J Clin Oncol*. 2002;20(24): 4713–4721.
18. Henningsson A, Karlsson MO, Viganò L, Gianni L, Verweij J, Sparreboom A. Mechanism-based pharmacokinetic model for paclitaxel. *J Clin Oncol*. 2001;19(20):4065–4073.
19. Huizing MT, Keung AC, Rosing H, et al. Pharmacokinetics of paclitaxel and metabolites in a randomized comparative study in platinum-pretreated ovarian cancer patients. *J Clin Oncol*. 1993; 11(11):2127–2135.
20. Huizing MT, Vermorken JB, Rosing H, et al. Pharmacokinetics of paclitaxel and three major metabolites in patients with advanced breast carcinoma refractory to anthracycline therapy treated with a 3-hour paclitaxel infusion: a European Cancer Centre (ECC) trial. *Ann Oncol*. 1995;6(7):699–704.
21. Wilson WH, Berg SL, Bryant G, et al. Paclitaxel in doxorubicin-refractory or mitoxantrone-refractory breast cancer: a phase I/II trial of 96-hour infusion. *J Clin Oncol*. 1994;12(8):1621–1629.
22. Nyman DW, Campbell KJ, Hersh E, et al. Phase I and pharmacokinetics trial of ABI-007, a novel nanoparticle formulation of paclitaxel in patients with advanced nonhematologic malignancies. *J Clin Oncol*. 2005;23(31):7785–7793.
23. Sparreboom A, Scripture CD, Trieu V, et al. Comparative preclinical and clinical pharmacokinetics of a Cremophor-free, nanoparticle albumin-bound paclitaxel (ABI-007) and paclitaxel formulated in Cremophor (Taxol). *Clin Cancer Res*. 2005;11(11): 4136–4143.
24. Biakhov MY, Kononova GV, Iglesias J, et al. *nab*-Paclitaxel in patients with advanced solid tumors and hepatic dysfunction: a pilot study. *Expert Opin Drug Saf*. 2010;9(4):515–523.
25. Guan Z, Li QL, Feng F, et al. Superior efficacy of a Cremophor-free albumin-bound paclitaxel compared with solvent-based paclitaxel in Chinese patients with metastatic breast cancer. Asia Pac. *Asia Pac J Clin Oncol*. 2009;5(3):165–174.
26. Hersh EM, Del Vecchio M, Brown MP, et al. Phase 3, randomized, open-label, multicenter trial of *nab*-paclitaxel vs dacarbazine in previously untreated patients with metastatic malignant melanoma. *Pigment Cell Melanoma Res*. 2012;25(6):863.
27. LoRusso PM, Venkatakrishnan K, Ramanathan RK, et al. Pharmacokinetics and safety of bortezomib in patients with advanced malignancies and varying degrees of liver dysfunction: phase I NCI Organ Dysfunction Working Group Study NCI-6432. *Clin Cancer Res*. 2012;18(10):2954–2963.
28. Lyman GH, Lyman CH, Agboola O. Risk models for predicting chemotherapy-induced neutropenia. *Oncologist*. 2005;10(6):427–437.
29. Kearns CM, Gianni L, Egorin MJ. Paclitaxel pharmacokinetics and pharmacodynamics. *Semin Oncol*. 1995;22(3 suppl 6):16–23.
30. Gradishar WJ, Krasnojon D, Cheporov S, et al. Significantly longer progression-free survival with *nab*-paclitaxel compared with docetaxel as first-line therapy for metastatic breast cancer. *J Clin Oncol*. 2009;27(22):3611–3619.
31. Joerger M, Huitema AD, Huizing MT, et al. Safety and pharmacology of paclitaxel in patients with impaired liver function: a population pharmacokinetic-pharmacodynamic study. *Br J Clin Pharmacol*. 2007;64(5):622–633.

Supporting Information

Additional supporting information may be found in the online version of this article at the publisher's web-site.